

DOI: 10.1002/celc.201402077

Electrochemical Grignard Reagent Synthesis for Ionic-Liquid-Based Magnesium–Air Batteries

Daniel Luder^[a] and Yair Ein-Eli^{*[a, b]}

Metal–organic compounds are widely used in the production of fine chemicals and pharmaceutical agents. On large scales, the chemical production of Grignard reagents (GRs) with ether solvents is difficult. The electrochemical synthesis of GRs in ionic-liquid-based electrolytes is reported herein. The electrochemical synthesis and presence of the GR product are demonstrated by cyclic voltammetry and ¹H nuclear magnetic resonance spectroscopy and by comparing the measured passing

charge to the final GR concentration. Additionally, the high-boiling ether tetraethylene glycol dimethyl ether is shown to be a suitable substitute for volatile tetrahydrofuran ether, which is currently used. A mechanism for the electrochemical synthesis of the GR is suggested and discussed, and the potential importance of the process for high-energy-density applications is demonstrated with a magnesium–air cell. Electropolishing of the Mg anode is also observed and discussed.

1. Introduction

Some of the most widely used materials in the chemical and pharmaceutical industries are metal–organic compounds. One of the most common types of such metal–organic compounds is the Grignard reagent (GR), which is generally formed by the reaction of an organic halide with Mg.^[1] GRs are used in numerous reactions involving C–C bond formation in these industries. Examples include the synthesis of organotin compounds^[2] used as stabilizers for vinyl chloride resins, catalysts for hardening urethane, and other industrial purposes. Additionally, GRs are used in many other branches of the chemical industry, including in the production of organosilicon products,^[3] organophosphorus compounds used for vitamin synthesis,^[4] and organoboron compounds used for conjugated polymer synthesis.^[5] GRs have many other uses: they are employed in the production of tamoxifen derivatives used in the pharmaceutical industry,^[6] they are used as flavor enhancers in the food industry in the form of maltol and ethyl maltol, and they are used in various anti-inflammatory analgesics such as Naproxen and in pharmaceuticals for pain treatment such as propoxyphene.^[6] In recent years, organomagnesium compounds have also been included in electrolytes of novel magnesium batteries,^[7,8] which are promising energy-storage systems with high energy densities.^[9] One of the important issues in GR synthesis is the synthesis of the solvent media, which plays an im-

portant role in the formation of the GR. Typically, the most suitable solvents are ethers,^[11] the most commonly used are tetrahydrofuran (THF) and diethyl ether. Practically, the production of a GR is challenging, as the surface of Mg is usually covered with a layer of hydroxides and oxides^[6] that impair the reaction of Mg with organic halides.^[11] In particular, if Mg is in contact with different organic media, a nonconductive passivation layer is present, which slows down or completely prevents chemical and electrochemical reactions that would otherwise occur in its absence.^[10,11] To overcome this, different initiating methods have been introduced to the synthesis procedure, such as the use of heat, environmental dryness, and chemical initiators (e.g. iodine, mercury, other GRs, Vitride, etc.).^[6] The physical form of Mg is also very important, as the ratio of surface to volume is an important factor; turnings, powders, and chips have been used as the Mg source due to high reactivity or ease of use.^[6] Elsewhere, it has been speculated that GRs may be formed if the magnesium is polarized in ethers containing GR precursors,^[10] but until recently, no substantial evidence of this has been found or presented.

Lately, we introduced a new route for the electrochemical synthesis of GRs in room-temperature ionic liquids (RTILs) without the need of a catalyst.^[12] It was demonstrated that GRs could be formed in situ through anodic polarization of Mg metal in a solution containing precursors of the GR reagent, with the chosen RTIL. Herein, we present and demonstrate our in-depth studies on the in situ electrochemical synthesis of the EtMgBr GR in nonaqueous ionic-liquid media by using electrochemical and spectroscopic methods, and we further report on the application of this process to batteries and electropolishing.

[a] D. Luder, Prof. Y. Ein-Eli

The Nancy and Stephen Grand Technion Energy program
Technion - Israel Institute of Technology, Haifa 3200003 (Israel)
Fax: +972-77-8871977

[b] Prof. Y. Ein-Eli

Department of Materials Science and Engineering
Technion - Israel Institute of Technology, Haifa 3200003 (Israel)
Fax: +972-4-829-4588
E-mail: eineli@technion.ac.il

 Supporting Information for this article is available on the WWW under <http://dx.doi.org/10.1002/celc.201402077>.

1.1 Room-Temperature Ionic-Liquid-Based Electrolyte

The electrolyte media used is based on RTILs that were researched seriously for the past two decades as electrolyte media.^[13–16] Generally, these solvents are liquids at room temperature and are purely composed of ions; the positive species is typically an organic, bulky, and asymmetric charged cation. Examples include derivatives of pyrrolidinium, imidazolium, pyridinium ammonium, and phosphonium.^[17–19] The negative species is an organic or inorganic charged anion ranging from a simple halide to the larger and charge-delocalized trifluoromethanesulfonate (triflate) and bis(trifluoromethylsulfonyl)imide (TFSI) anions.^[17,18] These liquids are advantageous for many existing and potential applications owing to their characteristics, such as chemical and thermal stability, a wide electrochemical window,^[17] high conductivity, low vapor pressure, no flammability, environmental friendliness, general nontoxicity, and the ability to tweak different properties by minutely adding or subtracting functional groups on the cation.^[17] Thanks to these properties, RTILs have found many applications in diverse areas such as bioscience, CO₂ capture, organic synthesis, and energy management.^[20] In particular, a large number of uses have been found in electrochemistry for applications such as electrodeposition, batteries, fuel cells, solar cells, and capacitors.^[21–24] In the area of Mg electrochemistry, certain nonacidic ionic liquids such as [1-butyl-1-methylpyrrolidinium bis(trifluoromethylsulfonyl)imide] (BMPTFSI) and [N,N-diethyl-N-methyl-N-(2-methoxyethyl) ammonium bis(trifluoromethanesulfonyl)imide] (DEMETFSI) have been found to be suitable as cosolvents for externally added GRs such as phenylmagnesium bromide (PhMgBr) and ethylmagnesium bromide (EtMgBr).^[14,16]

In the current study, an RTIL-based electrolyte is applied for the electrochemical organic synthesis of the EtMgBr GR. The electrolyte is composed of BMPTFSI, bromoethane (EtBr) as the GR precursor, and THF as a product stabilizer, which is a common and less volatile ether than alternatives such as diethyl ether. We also show that the high-boiling ether tetraethylene glycol dimethyl ether (TEGDME, b.p. 270 °C) can be used as a substitute for THF. During the reaction, Mg dissolves at the electrode surface after the application of a positive potential and reacts with EtBr to form the final GR product without the presence of any chemical catalysts.

The potential importance of the process for future high-energy-density applications in research and development is shown by using the electrolyte in the discharge of a magnesium–air cell. Additionally, a parallel magnesium electropolishing phenomenon is discussed.

2. Results and Discussion

2.1 Cyclic Voltammetry Studies and Electrochemical Window Evaluation

For electrochemical processes in general, particularly those requiring dryness, it is desirable to use nonaqueous electrolytes with wide electrochemical windows. Figure 1a presents the

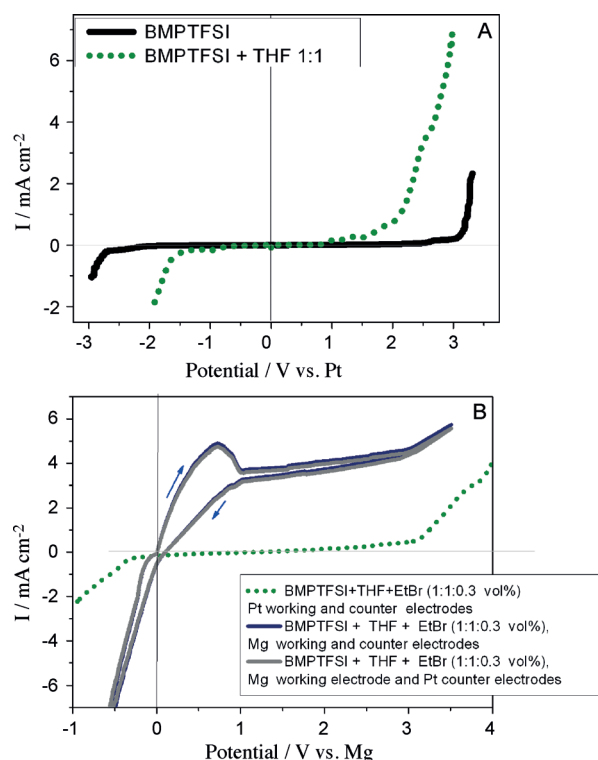


Figure 1. A) CV curves illustrating the electrochemical window of the ionic liquid BMPTFSI and of BMPTFSI + THF (1:1 v/v). Pt served as both the working and counter electrodes. B) CV of a cell employing a magnesium working electrode in BMPTFSI + THF + EtBr (1:1:0.3 v/v) electrolyte with a platinum counter electrode (gray) and a magnesium counter electrode (blue). BMPTFSI + THF + EtBr (1:1:0.3 v/v) with Pt as both working and counter electrodes (green dashed). Scan rate employed in all CVs was 5 mV s⁻¹.

electrochemical windows of BMPTFSI and an electrolyte composed of BMPTFSI + THF (1:1 v/v).

A particularly wide electrochemical window of about 5.5 V can be observed for BMPTFSI. This result is in good agreement with previous studies,^[18] which makes it advantageous as a stable electrolyte cosolvent for the synthesis of GRs, together with its other general advantages such as chemical and thermal stability and low vapor pressure.^[17] The presence of THF in the solution should stabilize the GR product^[6] and increase the conductivity of the electrolyte.^[14] It is, however, observable from Figure 1a that the addition of THF in 1:1 volume ratio with BMPTFSI narrows the electrochemical window of the solution by about 1.9 V.

To synthesize EtMgBr, a cell was assembled with the BMPTFSI + THF + EtBr (1:1:0.3 v/v) electrolyte. Figure 1b presents the results of two cyclic voltammetry (CV) experiments conducted with the mentioned cell and electrolyte; the working electrode was Mg, and the counter electrode was Pt and Mg in two separate CV experiments (anodic direction first). The electrochemical window of the electrolyte is presented for comparison.

In contrast to expectations with organic electrolytes, upon activation of the CV experiment no anodic or cathodic reaction overpotential was observed;^[10] the anodic reaction occurred immediately with the application of a potential and no evi-

dence of any Mg passivation layer was observed despite the fact that the Mg anode was immersed in an organic medium. This is despite the usual characteristic presence of a nonconductive passivating layer that inhibits the charge transport,^[10] even if the surface is only exposed to an inert atmosphere before immersion. This can be explained by interaction of the Mg surface with this specific electrolyte, which is different in manner than that with other organic solvents with or without magnesium salts, mainly through the reactivity of Mg to EtBr, as hypothesized and explained elsewhere.^[10]

It can be concluded from the curves presented in Figure 1 b that chemically reversible dissolution and deposition of Mg in the electrolyte occurs upon the application of the cyclic scanning. The deposition of Mg back onto the working electrode without electrolyte decomposition occurs only up to a low overvoltage of about 300 mV. The dissolution of Mg occurs without a parallel reaction involving the decomposition of the electrolyte. The corrosion current is derived from linear fitting of both the anodic and cathodic potentiodynamic profiles (a Tafel fit and potentiodynamic curves are shown in Figure 2) by using the same cell and electrolyte as that described above.

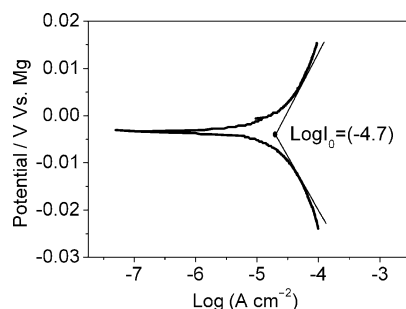


Figure 2. Anodic and cathodic potentiodynamic polarization profiles and affiliated linear polarization fitting of Mg working electrode in BMPTFSI + THF + EtBr (1:1:0.3 v/v) electrolyte. Mg metal served as a counter electrode and the scan rate employed was 5 mV s^{-1} .

The observed corrosion current was approximately $20 \mu\text{m cm}^2$. It was also found that the corrosion rate did not change substantially after different time intervals or after conducting additional CV experiments.

2.2 Potentiostatic Process and Analysis by using NMR Spectroscopy

To synthesize EtMgBr with a controlled concentration, a continuous constant potential of 0.2 V versus Mg was applied to a cell by utilizing Mg working and counter electrodes (electrolyte: BMPTFSI + THF + EtBr = 1:1:0.3 v/v), whereas the total charge passed through was calculated to be 0.805 C. The potentiostatic (current transient) curve is presented in Figure 3.

To determine the molecular structure of the species including the dissolved Mg, ^1H NMR spectroscopy was used as a useful analytic tool, as Mg is part of an organometallic structure^[25] such as the proposed electrochemical EtMgBr product.

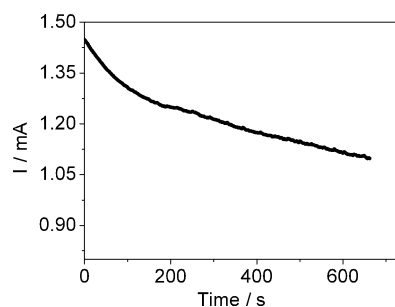


Figure 3. Potentiostatic synthesis of EtMgBr with a controlled concentration at 0.2 V vs. Mg. Electrolyte used was BMPTFSI + THF + EtBr (1:1:0.3 v/v). Magnesium metal serves as both the working and counter electrodes.

Moreover, this technique offers the possibility to indirectly calculate the product concentration.

Figure 4a presents the ^1H NMR spectrum of the pyrrolidinium-based cation (1-butyl-1-methylpyrrolidinium) in the ionic liquid BMPTFSI after drying, and Figure 4b presents the spectrum of EtMgBr in THF (1.2 M). The molecular structures and signal assignments of the mentioned species are presented in Figure 4c. Once the location of the main signals was established, an external reference solution was prepared by mixing BMPTFSI with THF/EtMgBr (1.2 M EtMgBr in THF) in a volumetric ratio of 1:1. Figure 5 presents the ^1H NMR spectrum of the above solution. The structures and signal assignments of the molecules from this graph are also represented in Figure 4c.

As can clearly be seen, the spectral footprint of EtMgBr is observed at chemical shifts of $\delta \approx 0.53$ (triplet, J) and -1.39 ppm (quartet, K) upon taking into consideration the signal identities of BMPTFSI, THF, and EtMgBr from Figure 4a–c. The latter signal is most easily isolated and served as the method of detection and calculation for the mentioned GR. The ^1H NMR spectra of the electrolyte after a constant potential (potentiostatic) experiment (total charge transfer: 0.805 C, see Table S1 in the Supporting Information) are presented in Figure 6. The spectra include the same chemical shifts and H coupling as seen with the reference solution sample in Figure 5. More importantly, there is proof of the existence of EtMgBr in the solution after the potentiostatic experiment. This can be seen at $\delta = 0.57$ and -1.33 ppm in Figure 6a, which correspond to EtMgBr as previously seen for the reference solution (signals at $\delta = 0.53$ and -1.39 ppm in Figure 5); this can be seen more clearly in the expansion of the $\delta = 0.9$ to -1.6 ppm range in Figure 6b, in which the spectrum unequivocally belonging to EtMgBr is marked.

Given that THF is a relatively volatile ether (b.p. 66°C), an alternative high-boiling ether was also considered for this process. Figure 7 presents the ^1H NMR spectrum taken subsequent to a potentiostatic experiment conducted with the same electrolyte and cell as presented in Figure 6a,b; however, this time THF was replaced by TEGDME, an ether with a boiling point of 270°C (electrolyte: BMPTFSI + TEGDME + EtBr = 1:1:0.3 v/v, charge passed through cell: 0.441 C). The signal of the hydrogen atoms belonging to EtMgBr can be observed in the same manner as that observed in Figure 6b, for which the supporting ether was THF. Thus, this ether can be used instead of THF

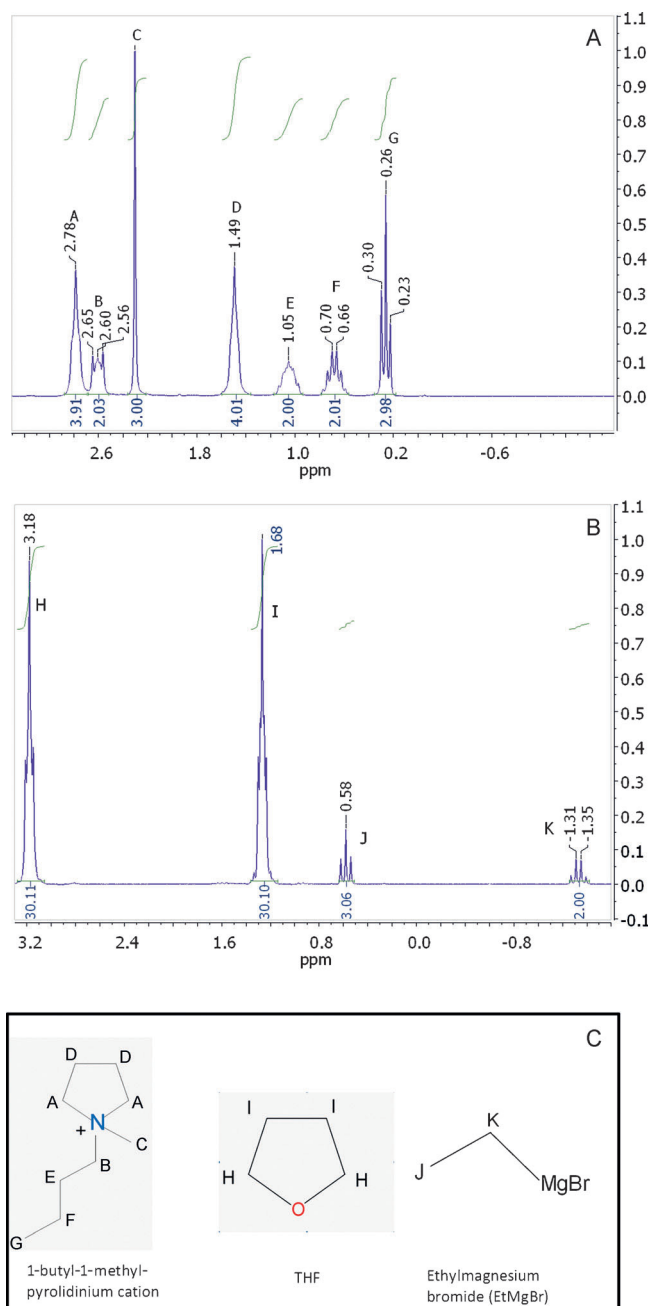


Figure 4. A) ^1H NMR spectrum of the pure BMPTFSI cation. B) ^1H NMR spectrum of 1.2 M EtMgBr in THF. C) Structure and signal assignment of the BMPTFSI cation, THF, and EtMgBr.

for cases in which ether evaporation disturbs the process, especially considering that GRs are strong bases and need species such as ethers to coordinate the magnesium atom in the product.^[6]

2.3 Charge-Concentration Dependence

A relation between the charge transferred during the potentiostatic experiments and the final concentration of the GR was determined by applying a constant potential of 0.2 V versus Mg at different lengths of time to a number of cells, and each

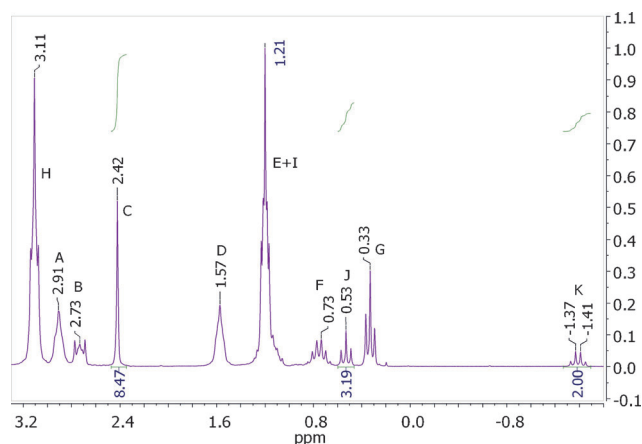


Figure 5. ^1H NMR spectrum of a reference solution prepared by mixing BMPTFSI and THF/EtMgBr (1.2 M) in a 1:1 v/v ratio.

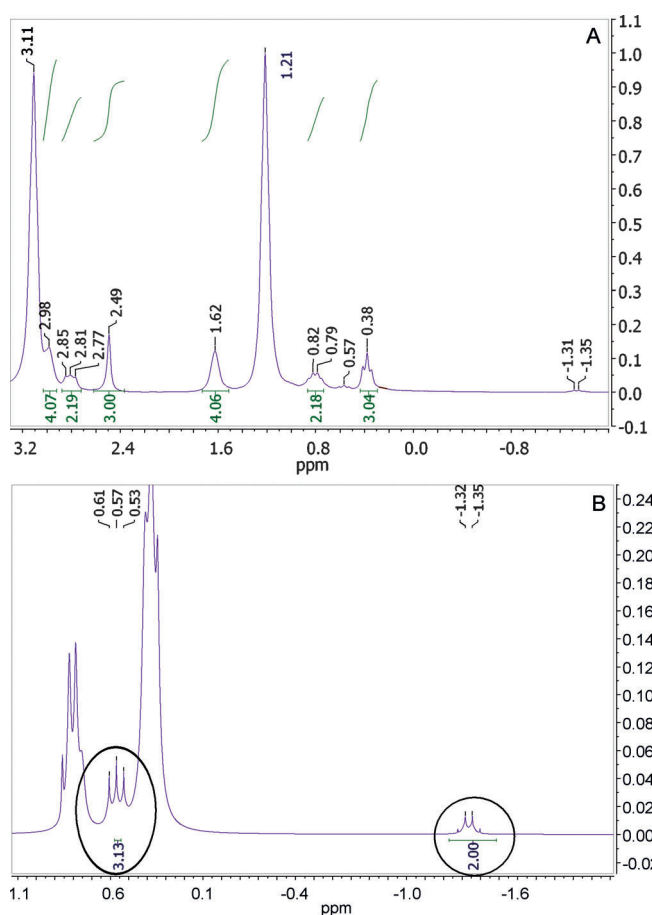


Figure 6. A) ^1H NMR spectrum obtained from a solution subsequent to a constant potential (potentiostatic) experiment with a total charge transfer of 0.805 C. B) Expansion of the ^1H NMR spectrum in the range from $\delta = 0.9$ to -1.6 ppm (hydrogen atoms belonging to EtMgBr are marked).

cell had a different value of total charge passing through it, as shown in Table S1.

The different EtMgBr concentrations in Table S1 were calculated by taking the relative integration of the signal at $\delta =$

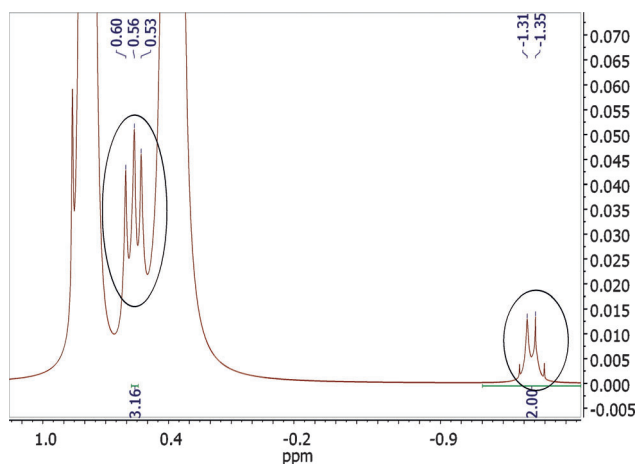


Figure 7. Expansion of the ^1H NMR spectrum obtained from a solution subsequent to a potentiostatic experiment. The electrolyte used was BMPTFSI + TEGDME + EtBr (1:1:0.3 v/v). The charge passed through the cell was 0.441 C (hydrogen atoms belonging to EtMgBr are marked).

–1.39 ppm belonging to the hydrogen on the “K” carbon atom in EtMgBr and the signal at $\delta=2.42$ ppm belonging to the hydrogen on the “C” carbon atom in the BMPTFSI cation (marked and presented in Figure 4a–c), as these two resonances are easily isolated. In the spectrum of the reference solution (Figure 5), it can be seen that the relative integration value is $2/8.51=0.235$, and this value is calibrated to the known EtMgBr concentration in the same solution (0.6 M). As an example, for the ^1H NMR spectroscopy results of the potentiostatic experiment presented in Figure 6a,b, the relative integration value is $2/26.58=0.0752$; according to the calibration method described above, this indicates an EtMgBr concentration of 0.192 M in the final solution.

The above concentration calculations were correlated with measurements conducted by volumetric titration of EtMgBr with 2-butanol. A 1 M solution of 2-butanol in toluene was titrated into the solution (diluted with THF and with the added colored indicator 2,2'-biquinoline) up to the point at which it changed color from red to yellow. After knowing the amount of titrated 2-butanol it was possible to calculate the amount and concentration of EtMgBr. Concentration results gained in this method were less accurate and deviated from the values in Table S1 by $\pm 10\%$; therefore, the concentrations were decided according to the more consistent spectroscopic method. Images of the solution before and after titration can be observed in Figure 8.

Figure 9 shows the linear dependence between the charge passed through the cell and the final concentration of EtMgBr. However, the final concentrations are higher than they should be if the reagents were synthesized as a result of an electrochemical current alone with 300 μL of solution (also indicated by the intercept), particularly if taking into account the corrosion current calculated previously when the cell was at rest.

To examine whether the GR synthesis is dependent on the application of a potential, a cell identical to the previous cells with THF was assembled, but no potential was applied to it.

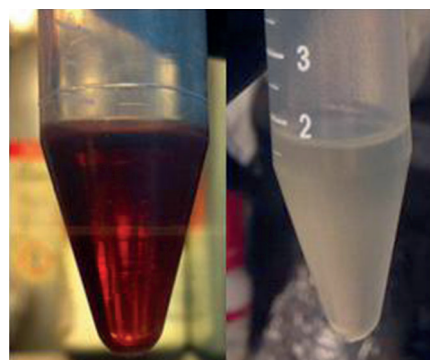


Figure 8. Solution prior to titration (left) and after titration (right) during the measurement of the concentration of EtMgBr by the volumetric titration method.

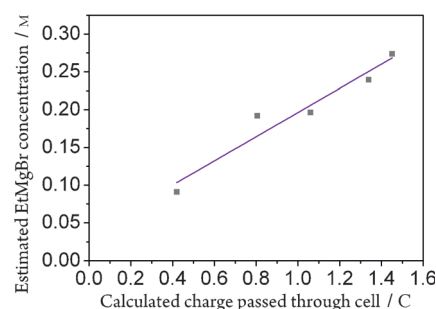


Figure 9. EtMgBr concentration versus charge passed through the cell in a constant potential (potentiostatic) mode of experiments.

The cell was filled with electrolyte and left to rest for 1500 s (more time than any other of the cells described previously). The ^1H NMR spectrum of the solution is presented in Figure 10. Identical results were obtained for electrolytes that were left to rest for 1 and 3 h. It can be seen that the signals of EtMgBr at $\delta=0.53$ (triplet, J) and -1.39 ppm (quartet, K), observed in the spectra in Figures 6 and 7, are missing. Consequently, without

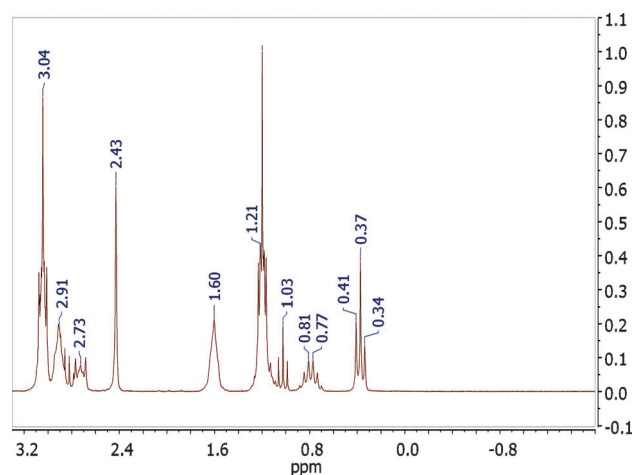


Figure 10. ^1H NMR spectrum of a solution prepared by mixing BMPTFSI, THF, and EtBr (1:1:0.3 v/v) after resting in the cell for 1500 s without potential application (cell was assembled with two magnesium electrodes only).

the application of a potential the reaction occurs at a rate negligible enough so that the reaction products are undetectable, even if the calculated corrosion is taken into account; it is suggested that this is due to the typical Mg passivation layer that prevents the chemical reaction from occurring at high rates.^[1,6,10] However, it has already been demonstrated that in this electrolyte the initial passivation layer necessitates an extremely small overpotential for dissolution or deposition.

2.4 Proposed Mechanism

One mechanism offered for the generation of GRs by involving Mg oxidation and alkyl halide reduction was suggested by Richey,^[6] formally named the “electrochemical corrosion hypothesis”,^[6] as illustrated in Figure 11. In this process, Mg is oxi-

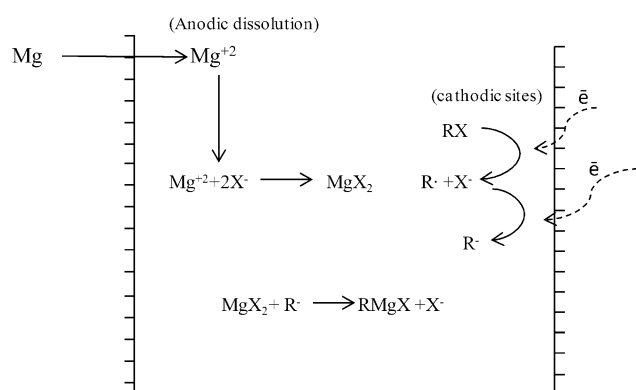


Figure 11. Suggested mechanism to describe in situ GR synthesis by electrochemical polarization.

dized and dissolved into the electrolyte and it coordinates then with halide anions (products of alkyl halide reduction) or TFSI anions from the electrolyte. Following Mg oxidation, the Mg ion species react with reduced alkyl species to form the GR. The high ionic conductivity^[14] of the electrolyte in the GR synthesis supports this process. The positive potential on the Mg anode supports Mg oxidation on the surface. The application of a potential can also be seen as an alternative catalyst for GR synthesis that could replace traditional catalyzing methods while at the same time controlling the amount of product synthesized. This mechanism can explain phenomena observed in similar systems.^[12]

2.5 Applications

The electrochemical synthesis of GRs described in previous sections has many potential applications; particularly if different RTILs and GR precursors are used according to the needed system properties. One important application can be made in the area of metal–air batteries,^[26–30] an important battery class due to very high theoretical energy densities^[31] that has potential applications in transport and energy storage for the grid. Particularly, GR synthesis can be applied in electrolytes for magnesium batteries. Many magnesium batteries in research

have electrolytes that include GRs or other organomagnesium species.^[7,25,32] The synthesis of GRs directly from the Mg anode into the electrolyte would not only create the desired active magnesium species, but it could also partly be used as the anodic reaction in the battery itself. One example is a magnesium–air cell^[33] with a magnesium anode, an electrolyte as mentioned in the Experimental Section, and a carbon-based air cathode to support ambient oxygen reduction. A discharge in such a cell is presented in Figure 12.

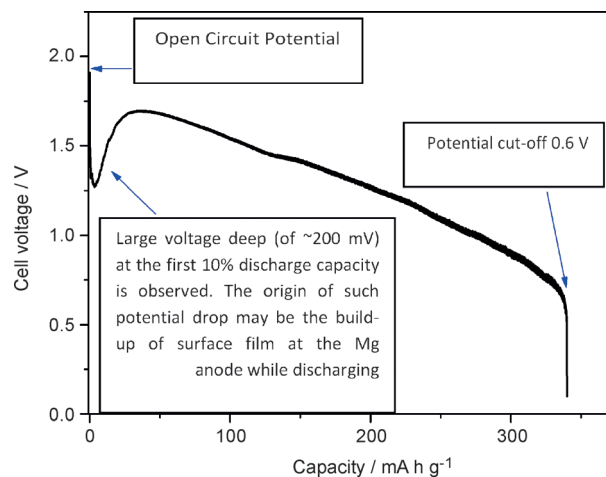


Figure 12. Discharge of a Mg–air cell with a Mg metal anode, a standard commercial air cathode (Electric-Fuel Ltd, Israel) by utilizing the electrolyte BMPTFSI + THF + EtBr (1:1:0.3 v/v). Current density applied in the cell discharge was 0.1 mA cm⁻².

A second application that would be relevant for the chemical industry is the controlled electrochemical synthesis of a GR in a flow reactor, followed by the optional reaction of the GR product with a controlled supply of an electrophilic reactant along the flow to afford the final desired product. In this way, the GR and its products could be synthesized in bulk while maintaining safety and controlled cost-effective mass production. A possible elaborate scheme is presented in Figure S1.

2.6 Magnesium Electropolishing Phenomenon

A separate interesting phenomenon was observed at the surface of Mg after the application of the CV experiment. The polished surface (polished up to P180 polish paper, 78 μm grit) was stripped to uniformity, and a mirrorlike, smooth surface remained. This phenomenon was tested in a separate experiment.

Figure 13 presents the CV curve of a cell and electrolyte identical to the cells prepared previously with THF, with a scan rate of 50 mV s⁻¹ (anodic direction first). High current densities can be observed together with typical anodic and cathodic reactions, as seen and discussed earlier. After CV, the Mg counter electrode was removed from the cell, cleaned with alcohol, and observed via scanning electron microscopy (SEM), as presented in Figure 14.

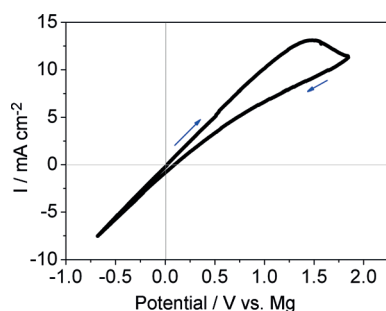


Figure 13. Cyclic voltammetry curve obtained at a scan rate of 50 mV s^{-1} . Magnesium metal served as both the working and counter electrodes. The electrolyte used was BMPTFSI + THF + EtBr (1:1:0.3 v/v).

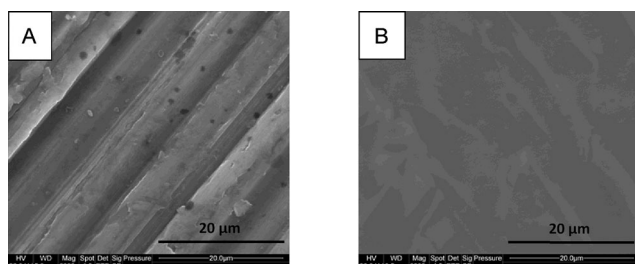


Figure 14. SEM image secondary electron contrast (SE) of the magnesium surface A) prior to and B) subsequent to polarization through application of CV.

The SEM images presented in Figure 14 are of secondary electrons (SE), which are characterized by providing a strong geometrical contrast. In Figure 14a, an Mg surface with clear roughness geometrical features can be seen after polishing, as mentioned earlier. Upon observing the same surface after CV, as seen in Figure 14b, it was very hard to obtain any contrast at all; this indicates the formation of an almost uniform and smooth surface unlike the roughly polished Mg surface before the experiment.

To gain more accurate surface data, atomic force microscopy (AFM) analysis was conducted on the same Mg surface. The surface morphology is presented in Figure 15. The average roughness (R_a) was 22 nm, and the root-mean-square roughness (R_q) was 27 nm.

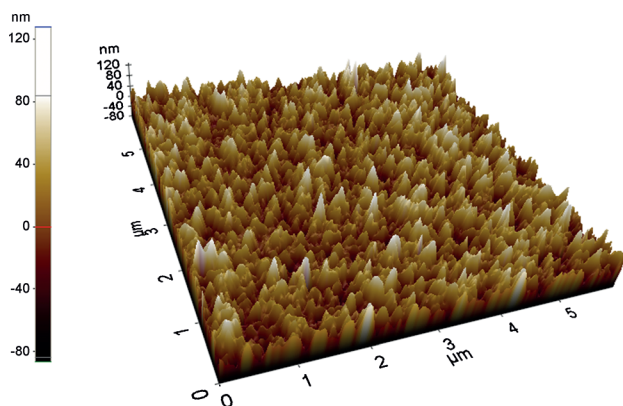


Figure 15. AFM image of the Mg surface after CV, as described in Figure 13.

The Mg surface after CV can be seen visually in Figure 16. It is suggested that this phenomenon is caused by the presence of a thin compact solid film that allows the transfer of cations while suppressing crystallographic etching on the surface.^[34] The above phenomena and underlining science will continue to be further studied.

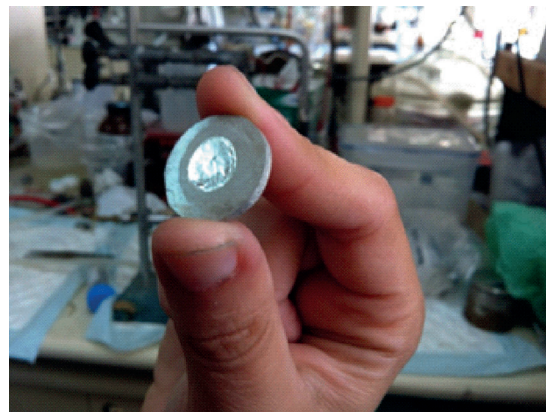


Figure 16. Mg surface after CV, as described in Figure 13.

3. Conclusions

Electrochemical synthesis of EtMgBr in ionic-liquid-based non-aqueous media was demonstrated by using electrochemical and spectroscopic methods. Spectroscopic evidence of EtMgBr was gained through the use of ^1H NMR spectroscopy. A linear dependence of the product concentration on the total charge passed was established by potentiostatic experiments conducted at different time intervals, and a process mechanism was suggested on the basis of the electrochemical corrosion hypothesis. In the electrolyte, it was shown that the high-boiling ether TEGDME could be used instead of low-boiling THF and that the same product was obtained. Importantly, it was demonstrated that the process could be applied in metal–air batteries, particularly magnesium–air batteries. More work is needed to better understand the surface chemistry developed at the Mg anode and air cathode surfaces. Spectroanalytical work, such as electrochemical impedance spectroscopy as well as in situ analysis of the developed surface film is planned. Additionally, Mg surface electropolishing was observed visually and by SEM and AFM, and this suggests a process involving cation transport through a compact film composed of oxidized magnesium and reduced solvent species.

These processes and phenomena could be used with numerous different reagents and parameters in myriad applications for the benefit of research and the pharmaceutical and chemical industries. Possible applications include industrial bulk GR synthesis in a controlled flowing framework, electrolyte synthesis for magnesium batteries before and during discharge, and Mg electropolishing for surface finishing or the preparation of smooth substrates.

Experimental Section

Electrolyte

BMPTFSI was purchased from loLiTec corp. (>99%) and dried under ultrahigh vacuum for 8 h ($H_2O < 10$ ppm). The water content was measured by Karl Fischer (KF) titration by using a 831 KF coulometer (Metrohm), and the sample was stored in an inert glove box (MBraun) with $H_2O/O_2 < 1$ ppm. EtBr (>99%) was purchased from Merck. THF, toluene, 2-butanol (>99.99%), and 2,2'-biquinoline were purchased from Sigma-Aldrich. Organic solvents were dried with 3 Å (8–12 mesh) silica-alumina molecular sieves and stored in a glove box ($H_2O < 20$ ppm, KF). The electrolyte was formed by mixing BMPTFSI, THF, and EtBr in a volumetric ratio of 1:1:0.3.

Cell

An illustration of the cell is presented in Figure S2 (electrolyte volume: 300 μ L) and was used in a three-electrode configuration. Pt foils (Sigma, >99.99%) and polished pure Mg (Dead Sea Works Corp., >99.8%) coin electrodes were used as working electrodes. Pt wires and Mg coin electrodes served as counter electrodes, whereas a polished pure Mg^[7,11,25,32] rod and Pt wire were used as reference electrodes. Pt electrodes were rinsed in nitric acid, washed, and dried before use. The Mg electrodes were mechanically polished, cleaned with acetone, dried with nitrogen, and finely polished and cleaned in an inert glove box before insertion in the cell; immediately afterwards, the electrolyte was inserted into the cell. All cyclic voltammograms or potentiostatic experiments were conducted in an inert glove box. Immediately upon completion of the experiment, the electrolyte was inserted into a standard NMR tube and analyzed by ¹H NMR spectroscopy. Standard commercial air electrodes (Electric Fuel Ltd.) were dried in a vacuum oven at 75 °C overnight and inserted into the glove box before use.

Equipment

Electrochemical studies were performed by using a 2273PAR EG&G potentiostat/galvanostat. Battery discharge was performed with an Arbin BT2000 cyler. A scanning electron microscope (FEI Quanta 200) equipped with an energy-dispersive X-ray spectroscopy system (EDS, Oxford Inst.) was utilized in surface morphology studies and chemical analysis. Before Mg surface analysis, the Mg electrodes were rinsed with ethanol and dried under nitrogen flow. ¹H NMR spectroscopy was conducted with a Bruker DPX 200 spectrometer; deuterium lock was established by inserting a separate Teflon capillary with deuterated methanol (MeOD) into the NMR tubes. AFM analysis was conducted with a XE-70 AFM analyzer (tapping mode, vertical resolution = 1 nm, lateral resolution 15 nm). Tip: NT-MDT silicon NSG 30.

Acknowledgements

The authors acknowledge support from the Nancy and Stephen Grand Technion Energy Program (GTEP).

Keywords: electrochemistry · electropolishing · Grignard reagent · ionic liquids · magnesium

- [1] M. B. Smith, J. March, *March's Advanced Organic Chemistry: Reactions, Mechanisms and Structure*, Wiley, New York, 2007.
- [2] M. J. Stoermer, J. T. Pinhey, *Molecules* **1998**, *3*, M67.
- [3] R. P. Narain, *Mechanisms in Organic Chemistry*, New Age International, New Delhi, 2008.
- [4] O. I. Kolodiazny, *Phosphorous Ylides, Chemistry and Application in Organic Synthesis*, Wiley-VCH, Weinheim, 1999.
- [5] K. Tanaka, Y. Chujo, *Macromol. Rapid Commun.* **2012**, *33*, 1235–1255.
- [6] *Grignard Reagents – New Developments* (Ed.: H. G. Richey, Jr.), Wiley, Chichester, 2000.
- [7] O. Mizrahi, N. Amir, E. Pollak, O. Chusid, V. Marks, H. Gottlieb, L. Larush, E. Zinigrad, D. Aurbach, *J. Electrochem. Soc.* **2008**, *155*, A103–A109.
- [8] Y. Gofer, O. Chusid, H. Gizbar, Y. Viestfrid, H. E. Gottlieb, V. Marks, D. Aurbach, *Electrochem. Solid-State Lett.* **2006**, *9*, A257–A260.
- [9] D. Aurbach, Y. Gofer, Z. Lu, A. Schechter, O. Chusid, H. Gizbar, Y. Cohen, V. Ashkenazi, M. Moshkovich, R. Turgeman, *J. Power Sources* **2001**, *97*, 28–32.
- [10] Z. Lu, A. Schechter, M. Moshkovich, D. Aurbach, *J. Electroanal. Chem.* **1999**, *466*, 203–217.
- [11] A. Meitav, E. Peled, *J. Electrochem. Soc.* **1981**, *128*, 825–831.
- [12] D. Luder, A. Kraysberg, Y. Ein-Eli, *ChemElectroChem.* **2014**, *1*, 362–365.
- [13] J. S. Wilkes, M. J. Zaworotko, *J. Chem. Soc., Chem. Commun.* **1992**, 965–967.
- [14] N. Yoshimoto, M. Matsumoto, M. Egashira, M. Morita, *J. Power Sources* **2010**, *195*, 2096–2098.
- [15] Y. NuLi, J. Yang, R. Wu, *Electrochem. Commun.* **2005**, *7*, 1105–10.
- [16] G. T. Cheek, W. E. O'Grady, S. Z. El Abedin, E. M. Moustafa, F. Endres, *J. Electrochem. Soc.* **2008**, *155*, D91–D95.
- [17] L. E. Barrosse-Antle, A. M. Bond, R. G. Compton, A. M. O'Mahony, E. I. Rogers, D. S. Silvester, *Chem. Asian J.* **2010**, *5*, 202–230.
- [18] J. Zhang, A. M. Bond, *Analyst* **2005**, *130*, 1132–1147.
- [19] B. Shvartsev, G. Cohn, H. Shasha, R. Eichel, Y. Ein-Eli, *Phys. Chem. Chem. Phys.* **2013**, *15*, 17837–17845.
- [20] M. Armand, F. Endres, D. R. MacFarlane, H. Ohno, B. Scrosati, *Nat. Mater.* **2009**, *8*, 621–9.
- [21] G. Cohn, D. Starosvetsky, R. Hagiwara, D. D. Macdonald, Y. Ein-Eli, *Electrochem. Commun.* **2009**, *11*, 1916–1918.
- [22] S. Lee, *Chem. Commun.* **2006**, 1049–1063.
- [23] G. Cohn, Y. Ein-Eli, *J. Power Sources* **2010**, *195*, 4963–4970.
- [24] G. Cohn, D. D. Macdonald, Y. Ein-Eli, *ChemSusChem.* **2011**, *4*, 1124–1129.
- [25] D. Aurbach, H. Gizbar, A. Schechter, O. Chusid, H. E. Gottlieb, Y. Gofer, I. Goldberg, *J. Electrochem. Soc.* **2002**, *149*, A115.
- [26] M. Balaish, A. Kraysberg, Y. Ein-Eli, *J. Electroanal. Chem.* **2013**, *707*, 85–88.
- [27] M. Balaish, A. Kraysberg, Y. Ein-Eli, *ChemElectroChem.* **2014**, *1*, 90–94.
- [28] M. Balaish, A. Kraysberg, Y. Ein-Eli, *Phys. Chem. Chem. Phys.* **2014**, *16*, 2801–2822.
- [29] K. Abraham, *ECS Trans.* **2008**, *3*, 67–71.
- [30] B. Kumar, J. Kumar, R. Leese, J. P. Fellner, S. J. Rodrigues, K. Abraham, *J. Electrochem. Soc.* **2010**, *157*, A50–A54.
- [31] F. Cheng, J. Chen, *Chem. Soc. Rev.* **2012**, *41*, 2172–2192.
- [32] N. Amir, Y. Vestfrid, O. Chusid, Y. Gofer, D. Aurbach, *J. Power Sources* **2007**, *174*, 1234–1240.
- [33] S. Sathyanarayana, N. Munichandraiah, *J. Appl. Electrochem.* **1981**, *11*, 33–39.
- [34] T. Hoar, D. Mears, G. Rothwell, *Corros. Sci.* **1965**, *5*, 279–289.

Received: March 31, 2014

Published online on June 27, 2014